Neurobiology of Disease

Atypical Gating Of M-Type Potassium Channels Conferred by Mutations in Uncharged Residues in the S_4 Region of KCNQ2 Causing Benign Familial Neonatal Convulsions

Maria Virginia Soldovieri,[1] Maria Roberta Cilio,[2] Francesco Miceli,[1] Giulia Bellini,[3] Emanuele Miraglia del Giudice,[4] Pasqualina Castaldo,[1] Ciria C. Hernandez,[5] Mark S. Shapiro,[5] Antonio Pascotto,[3] Lucio Annunziato,[1] and Maurizio Taglialatela[1,6]

[1]Section of Pharmacology, Department of Neuroscience, University of Naples Federico II, 80131 Naples, Italy, [2]Division of Neurology, Bambino Gesù Children's Hospital, 00165 Rome, Italy, Departments of [3]Child Neuropsychiatry, and [4]Pediatrics, Second University of Naples, 80138 Naples, Italy, [5]Department of Physiology, University of Texas Health Science Center, San Antonio, Texas 78229-3900, and [6]Department of Health Science, University of Molise, 86100 Campobasso, Italy

Heteromeric assembly of KCNQ2 and KCNQ3 subunits underlie the M-current (I_{KM}), a slowly activating and noninactivating neuronal K^+ current. Mutations in *KCNQ2* and *KCNQ3* genes cause benign familial neonatal convulsions (BFNCs), a rare autosomal-dominant epilepsy of the newborn. In the present study, we describe the identification of a novel *KCNQ2* heterozygous mutation (c587t) in a BFNC-affected family, leading to an alanine to valine substitution at amino acid position 196 located at the N-terminal end of the voltage-sensing S_4 domain. The consequences on KCNQ2 subunit function prompted by the A196V substitution, as well as by the A196V/L197P mutation previously described in another BFNC-affected family, were investigated by macroscopic and single-channel current measurements in CHO cells transiently transfected with wild-type and mutant subunits. When compared with KCNQ2 channels, homomeric KCNQ2 A196V or A196V/L197P channels showed a 20 mV rightward shift in their activation voltage dependence, with no concomitant change in maximal open probability or single-channel conductance. Furthermore, current activation kinetics of KCNQ2 A196V channels displayed an unusual dependence on the conditioning prepulse voltage, being markedly slower when preceded by prepulses to more depolarized potentials. Heteromeric channels formed by KCNQ2 A196V and KCNQ3 subunits displayed gating changes similar to those of KCNQ2 A196V homomeric channels. Collectively, these results reveal a novel role for noncharged residues in the N-terminal end of S_4 in controlling gating of I_{KM} and suggest that gating changes caused by mutations at these residues may decrease I_{KM} function, thus causing neuronal hyperexcitability, ultimately leading to neonatal convulsions.

Key words: **epilepsy; potassium channels; KCNQ2 subunits; benign familial neonatal convulsions; channel gating; mutations**

Introduction

Potassium (K^+) currents with distinct kinetic properties, modulation, and pharmacological profile are primary regulators of neuronal excitability (Shieh et al., 2000). The M-current (I_{KM}) is a low-threshold, slowly activating and deactivating, and noninactivating voltage-dependent K^+ current widely distributed in the peripheral nervous system (Brown and Adams, 1980) and in the CNS (Halliwell and Adams, 1982). I_{KM} plays a crucial role in repolarizing neuronal membrane potential after a depolarizing input, thus limiting repetitive firing and causing spike-frequency adaptation (Rogawski, 2000).

Received Feb. 9, 2007; revised March 16, 2007; accepted April 4, 2007.

This work was supported by grants from the Italian Ministry of the University and Research (COFIN 2003 and FIRB RBNE01XMP4), Telethon GP030209, European Commission STREP number 503038 (M.T.), and by the United States National Institutes of Health Grant RO1 NS043394 (M.S.S.). We are deeply indebted to Prof. Thomas J. Jentsch (Zentrum fur Molekulare Neurobiologie, Hamburg, Germany) for KCNQ2 and KCNQ3 cDNAs.

Correspondence should be addressed to Dr. Maurizio Taglialatela, Division of Pharmacology, Department of Neuroscience, School of Medicine, University of Naples Federico II, Ed. 19, Via Pansini 5, 80131 Naples, Italy. E-mail: mtaglial@unina.it.

DOI:10.1523/JNEUROSCI.0580-07.2007

 0270-6474/07/274919-10$15.00/0

K^+ channel subunits encoded by several genes of the *KCNQ* subfamily underlie I_{KM}, with KCNQ2 and KCNQ3 playing a major role at most neuronal sites. Mutations in *KCNQ2* (Biervert et al., 1998; Singh et al., 1998) or *KCNQ3* (Charlier et al., 1998), by reducing I_{KM} function, are responsible for benign familial neonatal convulsions (BFNCs), a rare autosomal-dominant idiopathic epilepsy of the newborn also known as benign familial neonatal seizures (Engel, 2001). BFNC-affected patients show multifocal or generalized tonic-clonic convulsions starting around the third day of postnatal life and disappearing spontaneously after a few weeks or months (Steinlein, 1998). Individuals affected by BFNC typically display normal psychomotor development, although a higher incidence of various epileptic manifestations later in life has been reported (Ronen et al., 1993). In addition to its pathophysiological role in BFNC, I_{KM} is emerging as a novel therapeutic target for CNS diseases; in fact, I_{KM} activators such as retigabine and flupirtine (Main et al., 2000; Rundfeldt and Netzer, 2000; Wickenden et al., 2000; Martire et al., 2004) appear as promising therapeutic tools against epilepsy (Rostock et al., 1996), pain (Blackburn-Munro and Jensen, 2003;

Passmore et al., 2003), anxiety (Korsgaard et al., 2005), dystonia (Richter et al., 2006), and neurodegenerative disorders (Otto et al., 2004; Boscia et al., 2006).

The study of the functional consequences of disease-causing mutations is of crucial relevance to define the pathophysiology of the disease and to design novel therapeutic strategies. Therefore, the aim of this work was to identify novel mutations responsible for BFNC in *KCNQ2* or *KCNQ3* genes and to study their consequences on I_{KM} function. In particular, we identified a novel missense mutation responsible for BFNC leading to an alanine to valine substitution at the N-terminal end of the voltage-sensing S_4 domain of KCNQ2 subunits (A196V; Q2 A/V). The consequences prompted by the A196V mutation on KCNQ2 subunit function were investigated by macroscopic and single-channel current analysis in a mammalian heterologous expression system; moreover, the functional properties of another previously described, but not functionally characterized, BFNC allele in which the KCNQ2 A196V mutation was associated to a leucine to proline substitution on the subsequent residue (L197P; Q2 AL/VP) (Moulard et al., 2001), were also evaluated.

The results obtained suggest that, albeit affecting uncharged residues, both the A196V and the A196V/L197P mutations introduced significant changes in channel sensitivity to voltage, revealing a previously unexplored functional role of these residues in KCNQ2 channel gating and highlighting their crucial involvement in BFNC pathophysiology. Furthermore, in both homomeric and heteromeric configuration with KCNQ3 subunits, the A196V mutation introduced an atypical dependence of current activation kinetics on the conditioning prepulse membrane voltage, a phenomenon never described previously. Such functional changes significantly decreased I_{KM} function, possibly leading to neuronal hyperexcitability and convulsive manifestations in BFNC-affected individuals.

Materials and Methods

Mutation analysis in KCNQ2 *and* KCNQ3 *genes.* Blood samples were taken with informed consent from all family members (see Fig. 1*A*). Total DNA was extracted from 5 ml of blood by the phenol/chloroform technique. All nucleotide numbers refer to the GenBank sequences NM_004518 (KCNQ2) and NM_004519 (KCNQ3). All exons of *KCNQ2* and *KCNQ3* were amplified as described previously (Miraglia del Giudice et al., 2000), using 17 and 15 sets of primers, respectively (sequences are available on request). Amplification was performed in a PE2400 Cycler (PerkinElmer, Foster City, CA) using 20 pmol of each primer and 0.4 U of *Taq* Gold DNA polymerase (Applied Biosystems, Foster City, CA) in 30 cycles with exon-specific annealing temperature. Mutation analysis was performed by direct sequencing of all exons with the Big Dye Terminator Cycle Sequencing Kit in an ABI PRISM 310 automated Sequencer (Applied Biosystems). Fifty healthy and unrelated control subjects were also checked for the presence of the mutation.

Mutagenesis of KCNQ2 cDNA and heterologous expression of wild-type and mutant KCNQ2 cDNAs. Mutations were engineered on human *KCNQ2* cDNA cloned into pcDNA3.1 by sequence overlap extension PCR with *Pfu* DNA polymerase, as described previously (Castaldo et al., 2002). Channel subunits were expressed in Chinese hamster ovary (CHO) cells by transient transfection. CHO cells were grown in 100 mm plastic Petri dishes in DMEM containing 10% fetal bovine serum, nonessential amino acids (0.1 mM), penicillin (50 U/ml), and streptomycin (50 μg/ml) in a humidified atmosphere at 37°C with 5% CO_2. For electrophysiological experiments, the cells were seeded on glass coverslips (Carolina Biological Supply Company, Burlington, NC) and transfected on the next day with the appropriate cDNAs using Lipofectamine 2000 (whole-cell recordings; Invitrogen, Milan, Italy) or Polyfect (single-channel recordings; Qiagen, Valencia, CA), according to the manufacturer's protocol. A plasmid encoding for enhanced green fluorescent protein (Clontech, Palo Alto, CA) was used as transfection marker; total cDNA in the transfection mixture was kept constant at 4 μg.

Whole-cell electrophysiology. Currents from CHO cells were recorded at room temperature (20–22°C) 1 d after transfection, using a commercially available amplifier (Axopatch 200A; Molecular Devices, Union City, CA) and the whole-cell configuration of the patch-clamp technique, with glass micropipettes of 3–5 MΩ resistance. The extracellular solution contained the following (in mM): 138 NaCl, 2 $CaCl_2$, 5.4 KCl, 1 $MgCl_2$, 10 glucose, and 10 HEPES, pH 7.4 with NaOH. The pipette (intracellular) solution contained the following (in mM): 140 KCl, 2 $MgCl_2$, 10 EGTA, 10 HEPES, 5 Mg-ATP, 0.25 cAMP, pH 7.3–7.4 with KOH. The pCLAMP software (version 6.0.4) was used for data acquisition and analysis.

To generate conductance–voltage (G/V) curves, the cells were held at −80 mV and then depolarized for 0.75–3 s from −80 to +20 mV using an incremental pulse of 10 mV, followed by an isopotential pulse at 0 mV of 350 ms; the current values recorded at the beginning of the 0 mV pulse were measured, normalized, and expressed as a function of the preceding voltages. The data were then fit to a Boltzmann distribution of the following form: $y = \max/[1 + \exp(V_{1/2} - V)/k]$, where V is the test potential, $V_{1/2}$ is the half-activation potential, and k is the slope factor; this method only gives a rough estimate of the number of gating charges displaced during channel activation. However, a more elaborate analysis (such as the use of multiple Boltzmann to fit the G/V data or the assessment of the limiting slope conductance) required complex measurements, which were hampered by the current tendency to rundown and by the slow time course of the currents to reach steady-state conditions, requiring several minutes to record families of currents scanning the entire voltage range using smaller (2–5 mV) voltage steps. To analyze current activation kinetics, the current traces recorded in response to incremental voltage steps were fitted to a double-exponential function of the following form: $y = amp_f \exp(-t/\tau_f) + amp_s \exp(-t/\tau_s)$, where amp_f and amp_s indicate the amplitude of the fast and slow exponential components, respectively, whereas τ_f and τ_s indicate the time constants of these components. When the prepulse voltage dependence of the activation kinetics were studied, the cells were subjected to a 3 s prepulse to potentials ranging from −100 to −40 mV, followed by an isopotential step at 0 mV; the currents recorded at 0 mV were then fitted to the previously described double-exponential function. TEA blockade was quantified by measuring the percentage of current inhibition produced by a 2 min application; the effects of retigabine were quantified by measuring the negative shift in the midpoint potential of activation after a 3 min drug exposure.

Single-channel electrophysiology. For single-channel recordings, channel activity in cell-attached patches was measured 48–96 h after transfection. Pipettes had resistances of 7–15 MΩ when filled with a solution of the following composition (in mM): 150 NaCl, 5 KCl, 2 $CaCl_2$, 1 $MgCl_2$, and 10 HEPES, pH 7.4 with NaOH. Cells were bath perfused with a solution containing the following (in mM): 175 KCl, 4 $MgCl_2$, and 10 HEPES, pH 7.4 with KOH to clamp the resting membrane potential near 0 mV. Recording and analysis methods were similar to those described previously (Selyanko and Brown, 1999; Li et al., 2004a,b). Currents were recorded using an Axopatch 1-D amplifier (Molecular Devices). The data were acquired with Pulse software (Bruxton, Seattle, WA), sampled at 5 kHz, and filtered at 500 or 200 Hz. Single-channel data were analyzed using PulseFit and TAC (Bruxton) software. Open and closed events were analyzed by using the "50% threshold criterion." All events were carefully checked visually before being accepted. Open probability (P_o) histograms were generated using TACFit (Bruxton). Our estimate of the total number of channels in a given patch is based on two common assumptions: (1) that all of the channels in a patch will behave in an identical manner (i.e., they are homogeneous) and (2) that the P_o of one channel does not depend on the gating state of the other(s) (i.e., they are independent). Under these reasonable assumptions, the presence of only one channel in a patch can be assumed if no superimposed openings are observed for a sufficiently long period of time that depends on the P_o of any given channel, and in the case of multiple channels in the patch, the number of open channels is governed by the binomial distribution (Horn, 1991). In our case, we evaluated the total number of channels in

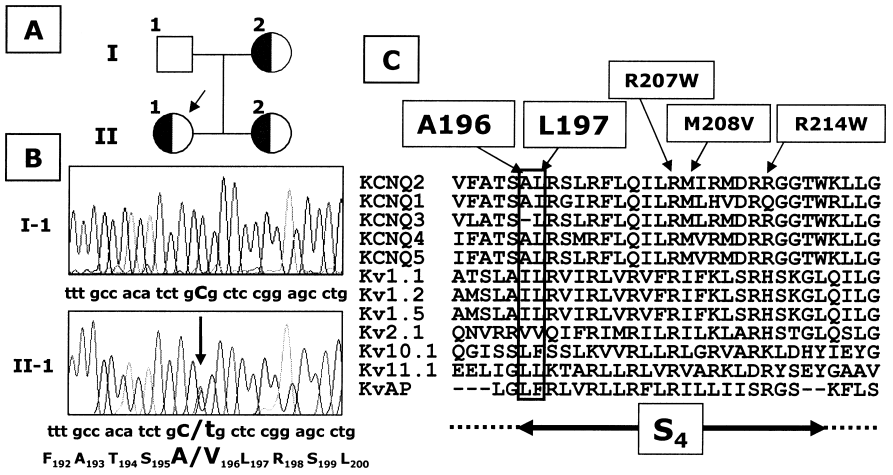

Figure 1. Genetic analysis of the BFNC family. ***A***, Pedigree of the family. The proband is indicated by an arrow. ***B***, Double-strand partial sequencing of KCNQ2 and deduced amino acid sequence in the unaffected (I-1) and BFNC-affected (II-1) individuals. The missense mutation c587t is indicated by an arrow. ***C***, Sequence alignment of the S_4 domain of the indicated potassium channel subunits (Clustal W; http://www.ebi.ac.uk/clustalw/); larger font sizes indicate the mutant residues investigated here. Previously described BFNC-associated mutations are indicated with smaller font sizes. The arrow at the bottom spans the S_4 segment, according to Aggarwal and MacKinnon (1996).

the patch by continuously recording for >1 min at strongly depolarized potentials, at which P_o is highest (>0.2). Using this method, we estimate a maximal error rate of 3.8%, which is within the error of the pooled measurements. When superimposed openings were observed, the total number of channels in the patch was estimated from the maximal number of superimposed openings. At any given potential, the single-channel amplitude (i) was calculated by fitting all-point histograms with single- or multi-Gaussian curves. The difference between the fitted "closed" and "open" peaks was taken as i. P_o/V relationships were fitted by a Boltzmann equation, and the single-channel conductance was obtained from the slope of the i/V chord fitted by linear regression using GraphPad Prism version 4.0 for Windows (GraphPad Software, San Diego, CA).

Statistics. Data are expressed as the mean ± SEM. Statistically significant differences between the data were evaluated with the Student's t test or with the ANOVA followed by the Student–Newman–Keuls test ($p < 0.05$).

Results

Clinical data

Individual II-1

The proband (Fig. 1*A*) is the first child of healthy, unrelated parents. She was born by C-section for podalic presentation at 39 weeks of gestation after an uneventful pregnancy; her birth weight was 2900 g, length was 47 cm, and head circumference was 36 cm. Apgar scores were 8/10 and 9/10 at 1 and 5 min, respectively. Tonic seizures started 2 d after birth, accompanied by short (1–3 min) but frequent periods of apnea and cyanosis, with normal interictal status. Analysis of serum, urine, and CSF were normal and ruled out metabolic disturbances or an infectious process. Ultrasound imaging of the brain was normal. The girl was treated with phenobarbital (PB) at a loading dose of 20 mg/kg, followed by a maintenance dose of 5 mg/kg. Seizures rapidly stopped. The child became mildly hypotonic for a few days and then completely recovered. At 2 months of age, she was seizure-free, had a normal psychomotor development, and her neurological examination was unremarkable. PB was gradually discontinued, but 10 d later she presented again with a cluster of seizures characterized by a diffuse hypertonia accompanied by apnea and cyanosis, followed by unilateral or bilateral clonic movements of the limbs. Seizures lasted for 1–3 min and repeated frequently over 2 d. Interictal electroencephalograms (EEGs) in the active phase showed focal abnormalities, spikes or sharp waves in the central regions. Brain magnetic resonance imaging was normal. PB was reintroduced leading to a rapid cessation of seizures. No additional seizures have been reported since then, despite treatment discontinuation at 8 months of age. At 5 years of age, she has a normal neurological development and EEG, and she remains seizure-free.

Individual II-2

The younger sister of the proband is a 13-month-old infant. She was born full-term after a normal pregnancy and delivery; on the second day of life, she suffered from brief repeated focal seizures. Extensive investigations including neuroimaging and metabolic tests were negative. Neurological evaluation was normal. Seizures were treated with carbamazepine with complete remission. An attempt of drug withdrawal at 8 months of age led to seizure relapse; she was then treated with carbamazepine until 1 year of age. At 13 months, she is seizure-free, the EEG is normal, and she shows normal psychomotor development.

Individuals I-1 and I-2

The mother of the proband (I-2) suffered from neonatal seizures. Seizures stopped within a few days but recurred afterward during the first year. She was therefore treated with PB and phenytoin until the sixth year of age. Since then, no additional seizure occurred, and she shows normal neurological exam and development. Neurological history was unremarkable for the father of the proband (I-1).

Molecular genetic analysis

KCNQ2 and *KCNQ3* gene mutation analysis performed on the index case revealed a heterozygous missense mutation (c587t) in *KCNQ2* (Fig. 1*B*), whereas no mutation was found in *KCNQ3*. The same KCNQ2 mutation was also found in the affected mother and sister of the proband, but not in the unaffected father and in 50 control subjects, consistent with the segregation of the phenotype. The c587t *KCNQ2* mutation leads to the substitution of the alanine at position 196 with a valine residue (A196V; Q2 A/V) (Fig. 1*B*); position 196 is located at the N-terminal end of the S_4 voltage sensor, before the first of the six positively charged arginines within this region (R198) (Fig. 1*C*). The alanine residue at this position is conserved among all KCNQ-type subunits, except for KCNQ3, where the corresponding residue is missing from the primary sequence. In most non-KCNQ K^+ channel subunits, hydrophobic residues (L, V, I) occupy this position. In another BFNC-affected family, Moulard et al. (2001) also described the same *KCNQ2* mutation in association, on the same allele, with a missense mutation affecting the subsequent highly conserved L residue, resulting therefore in the double mutation A196V+L197P (Q2 AL/VP).

Steady-state and kinetic properties of the macroscopic currents formed by KCNQ2, KCNQ2 A/V, and KCNQ2 AL/VP homomeric channels

To characterize the electrophysiological properties of the K^+ channels formed by the subunits carrying the described BFNC-

associated mutations, CHO cells were transfected with the cDNAs encoding for wild-type or mutant subunits, and the resulting currents were recorded by means of the whole-cell configuration of the patch-clamp technique.

Heterologous expression of KCNQ2 subunits led to the appearance of voltage-dependent K^+-selective currents characterized by a rather slow time course of activation and deactivation and a threshold for current activation around −60 mV (Fig. 2*A–C*). Functional voltage-dependent K^+ currents were also generated by channels composed of KCNQ2 subunits carrying the A196V or the A196V/L197P mutations; the density of these currents was identical in KCNQ2-, KCNQ2 A/V-, and KCNQ2 AL/VP-transfected cells, being, respectively, 35 ± 8, 37 ± 4, and 44 ± 6 pA/pF at +20 mV ($n = 7$ for each group; $p > 0.05$).

Homomeric channels carrying the A/V substitution in KCNQ2 exhibited a significant rightward shift in the midpoint potential for activation, with no concomitant change in the slope of the conductance–voltage curve (Fig. 2*B*). In fact, for KCNQ2 and KCNQ2 A/V homomeric channels, the $V_{1/2}$ were, respectively, −39.7 ± 1.2 and −16.6 ± 1.2 mV ($n = 10$ for each group; $p < 0.05$), whereas the k were, respectively, 10.7 ± 1.0 and 11.5 ± 0.9 mV/*e*-fold ($n = 10$ for each group; $p > 0.05$). Interestingly, significant changes in both the midpoint activation potential as well as in the slopes of the *G*/*V* curves were prompted by homomeric incorporation of the AL/VP double substitution; in fact, when conditioning depolarizing pulses of 750 ms were used to avoid excessive current rundown, the $V_{1/2}$ and the k of KCNQ2 and KCNQ2 AL/VP homomeric channels were −29.2 ± 1.0 and −5.7 ± 1.2 mV ($p < 0.05$), and 10.6 ± 0.8 and 14.5 ± 1.0 mV/*e*-fold ($p < 0.05$), respectively (Fig. 2*C*).

K^+ currents carried by homomeric channels composed of KCNQ2 and KCNQ2 A/V subunits displayed activation kinetics, which were adequately fitted by a sum of two exponential functions (Fig. 2*D*) (Wang et al., 1998; Castaldo et al., 2002), with no noticeable difference in the fast or slow time constants (τ_f and τ_s, respectively) between the two channels. For KCNQ2 homomeric channels, at any given potential above −40 mV, the relative amplitude of the fast component, called A_f, largely dominated over that of the slow component, called A_s; thus, the ratio of A_f and A_s, expressed as $A_f/A_f + A_s$, was >80% at all potentials investigated (Fig. 2*E*). In contrast, in KCNQ2 A/V homomeric channels, the $A_f/A_f + A_s$ ratio was significantly decreased for potentials higher than or equal to −20 mV (Fig. 2*E*), suggesting that the relative amplitude of the slow component A_s assumed a progressively increasing weight with stronger depolarizations.

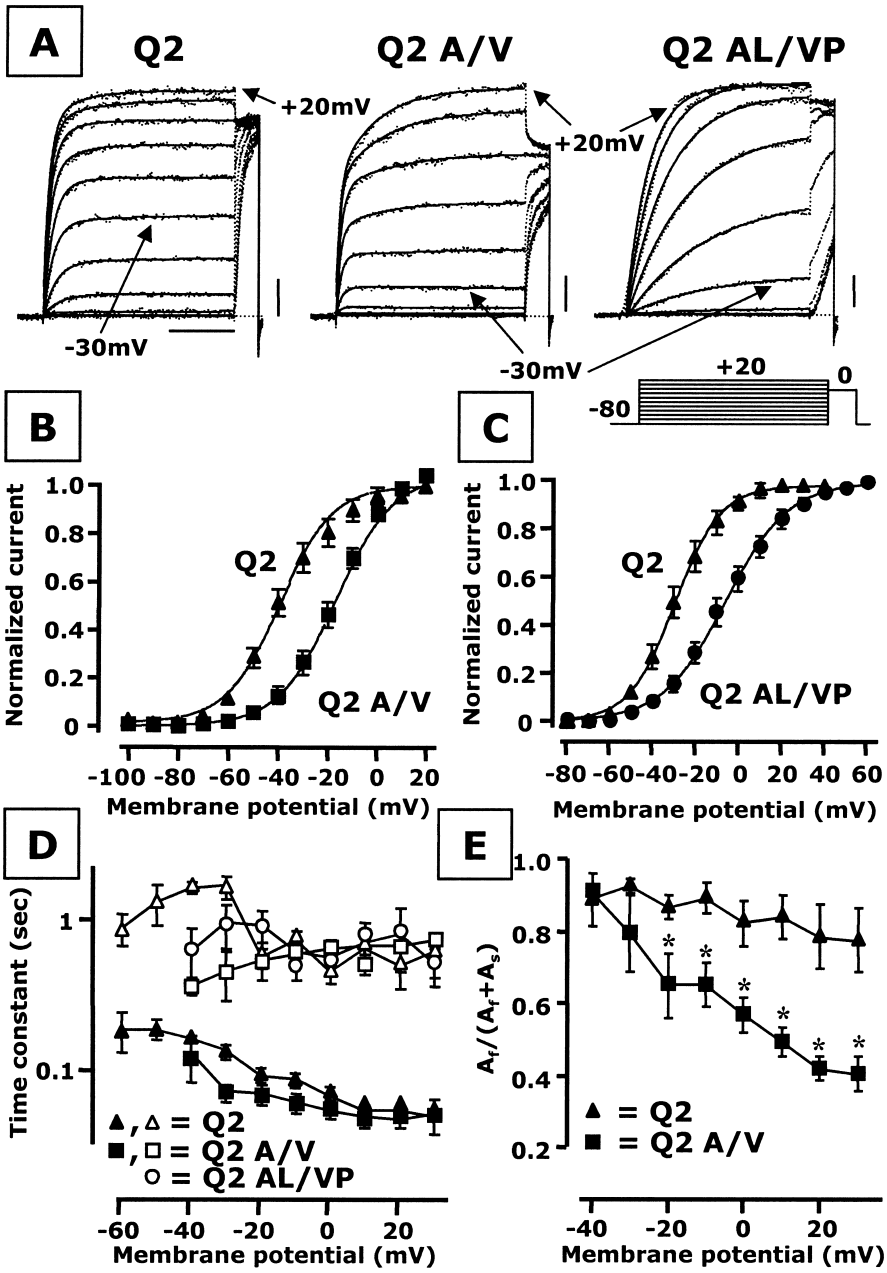

Figure 2. Steady-state and kinetic properties of the macroscopic currents carried by KCNQ2, KCNQ2 A/V, and KCNQ2 AL/VP homomeric channels. ***A***, Representative current traces elicited by KCNQ2 (Q2), KCNQ2 A/V (Q2 A/V), and KCNQ2 AL/VP (Q2 AL/VP) channels recorded from transiently transfected CHO cells in response to depolarizing pulses of 10 mV increments from −80 to +20 mV from a −80 mV holding potential (current scale, 200 pA; time scale, 1 s). Solid lines represent single-exponential (Q2 AL/VP) or double-exponential (Q2, Q2 A/V) fits of the current traces. ***B***, ***C***, Steady-state activation curves of Q2 and Q2 A/V channels (***B***; 3 s conditioning pulses) or Q2 and Q2 AL/VP channels (***C***; 0.75 s conditioning pulses). Continuous lines represent Boltzmann fits of the experimental data. ***D***, Activation time constants obtained by fitting to a biexponential function the current traces from Q2, Q2 A/V, and Q2 AL/VP channels. Open symbols, Slow time constants; filled symbols, fast time constants. ***E***, Relative amplitudes of the fast and slow current activation components, expressed as $A_f/A_f + A_s$, for Q2 and Q2A/V channels as a function of membrane voltage. Asterisks denote Q2 A/V values significantly different from the corresponding Q2 values ($p < 0.05$).

The activation kinetics of the K^+ currents flowing through KCNQ2 AL/VP homomeric channels were dramatically slowed down when compared with those of KCNQ2 channels, with a complete ablation of the fast component of current activation; thus, in the voltage range between −40 and +20 mV, KCNQ2 AL/VP current activation kinetics were properly fitted by a single-

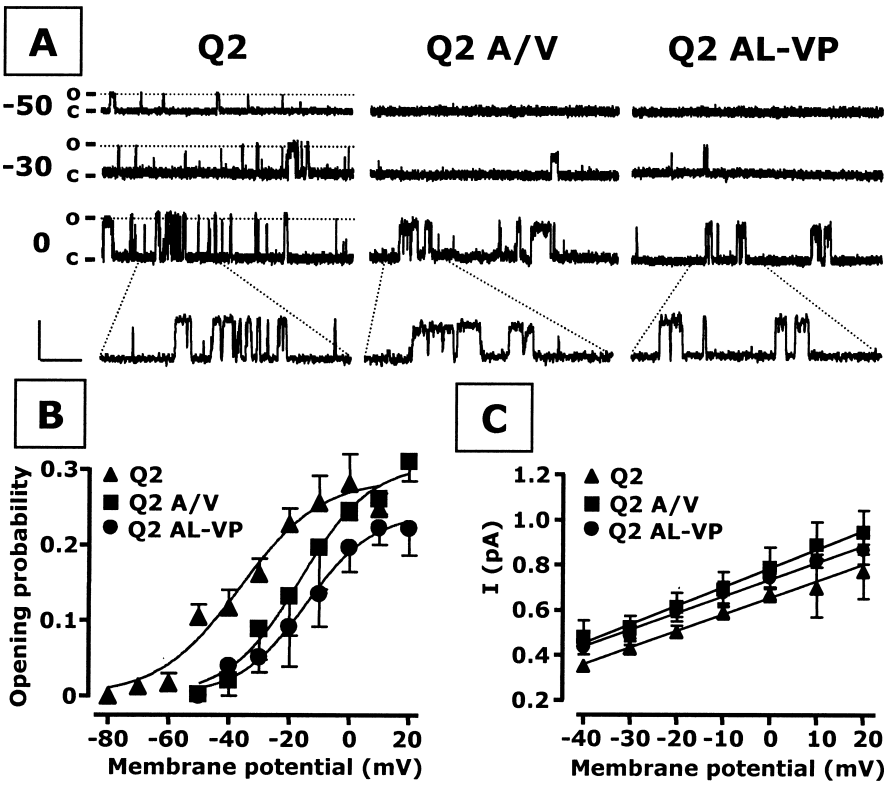

Figure 3. Single-channel properties of KCNQ2 (Q2), KCNQ2 A/V (Q2 A/V), and KCNQ2 AL/VP (Q2 AL/VP) homomeric channels. ***A***, Representative single-channel sweeps obtained at the membrane potentials indicated on the left. The current levels for the closed (C) or the open (O) state are also indicated on the left. Amplitude scale, 1 pA; time scale, 500 ms (200 ms in the enlarged views). ***B***, Single-channel P_o/V curves of KCNQ2, KCNQ2 A/V, and KCNQ2 AL/VP homomeric channels; continuous lines are Boltzmann fits of the experimental data. ***C***, Unitary current–voltage relationships of single KCNQ2, KCNQ2 A/V, and KCNQ2 AL/VP channels. Straight lines represent linear fits of the experimental data; each data point was calculated from four to eight patches.

exponential function having time constants identical to those of τ_s of both KCNQ2 and KCNQ2 A/V channels (Fig. 2*D*).

The described mutations did not alter channel selectivity for K^+ over Na^+ ions because no changes were observed in the macroscopic current reversal potential (V_{rev}) measured in our recording conditions for KCNQ2, KCNQ2 A/V, and KCNQ2 AL/VP homomeric channels (V_{rev} was -78.8 ± 2 mV, -75.2 ± 2.1 mV, and -76.8 ± 2, respectively for the three channels; $n = 4–6$; $p > 0.05$ against each other).

Single-channel analysis of the currents carried by KCNQ2, KCNQ2 A/V, and KCNQ2 AL/VP homomeric channels

Given the interesting effects on macroscopic gating seen in the KCNQ2 A/V and AL/VP mutants, we then decided to examine the channels at the single-channel level. In particular, we ascertained whether the shifts in voltage dependence produced by the mutations observed in whole-cell recordings would be reflected in parallel effects on the voltage dependence of channel open probabilities. To this aim, because currents carried by KCNQ-type subunits undergo strong modulation by intracellular as well as membrane-associated molecules (Marrion, 1997), we used the cell-attached configuration for single-channel recordings, to avoid possible perturbation of the intracellular milieu and retain intact the biochemical machinery required for I_{KM} modulation. Figure 3*A* shows typical recordings obtained from CHO cells transfected with KCNQ2, KCNQ2 A/V, and KCNQ2 AL/VP cDNAs at various values of membrane potentials (-50, -30, and 0 mV). Openings of KCNQ2 channels were consistently observed at -50 mV; in contrast, openings of homomeric channels carrying both A/V and AL/VP mutations were never observed at -50 mV but were only detected at more positive membrane potentials (higher than or equal to -30 mV). When computing the averaged probability of opening at each potential for several patches, we obtained the single-channel P_o/V curves described in Figure 3*B*, which were then fitted to the same form of the Boltzmann distribution described previously. The maximal open probability of homomeric KCNQ2 channels was 0.29 ± 0.04; this maximal value was not affected by the A/V or the AL/VP mutations (0.29 ± 0.01 and 0.25 ± 0.02, respectively; $n = 4–8$). However, both mutations caused an ~20 mV rightward shift in the midpoint potential for activation (KCNQ2, -36.3 ± 5.1 mV; KCNQ2 A/V, -16.4 ± 5.0 mV; KCNQ2 AL/VP, -14.5 ± 6.6 mV; $n = 4–8$; $p < 0.05$), with no concomitant modification of the slope value (KCNQ2, 13.4 ± 4.9 mV/*e*-fold, KCNQ2 A/V, 11.7 ± 3.8 mV/*e*-fold; KCNQ2 AL/VP, 11.1 ± 5.1 mV/*e*-fold; $n = 4–8$). Finally, despite these marked changes in opening voltage dependence, the single-channel conductance for K^+ ions was not affected by the mutations, being 7.4 ± 0.8, 8.3 ± 1.4, and 7.4 ± 0.9 pS for KCNQ2, KCNQ2 A/V, and KCNQ2 AL/VP channels, respectively ($n = 4–8$).

Current activation kinetics of KCNQ2 A/V channels depend on the prepulse voltage

Activation kinetics of the K^+ conductance in the squid axon depend on the potential of conditioning prepulses, such that activation is slower with more hyperpolarized conditioning pulses (Cole and Moore, 1960). This "Cole-Moore effect" is thought to be attributable to the driving of the channels into deeper closed states at more negative voltages, thus requiring more time to reach the open state after depolarization. Current activation kinetics of homomeric KCNQ2 channels were insensitive to changes in the preceding voltages; Figure 4*A* shows representative KCNQ2 current traces at 0 mV recorded after 3 s conditioning pulses to -100 or -60 mV, as indicated. At 0 mV, τ_f, τ_s, and their amplitude ratio $A_f/A_f + A_s$ were not significantly different when conditioning pulse potentials between -100 and -40 mV were used (Figs. 4*B*,*C*). Unexpectedly, we observed a striking effect of conditioning pulse potential for the KCNQ2 A/V mutant that is the inverse of the Cole-Moore effect. Indeed, the activation kinetics of KCNQ2 A/V homomeric channels were markedly slower when the 0 mV test pulse was preceded by more depolarized (higher than or equal to -80 mV) conditioning pulses (Fig. 4*A*). We analyzed this effect as in Figure 2 both in terms of alterations in τ_f and τ_s and in their amplitude ratios. In KCNQ2 A/V channels, τ_f appeared to be unaffected by the conditioning prepulse voltage. In contrast, in the same channels, a -60 mV conditioning prepulse significantly increased τ_s value at 0 mV (Fig. 4*B*); the largest effect was on the relative amplitude ratio $A_f/A_f + A_s$, which, for KCNQ2 A/V but not KCNQ2 channels, became

increasingly smaller (smaller τ_f fraction), with more depolarized prepulses (Fig. 4*C*).

Interestingly, the introduction of the L197P mutation into the A196V background seemed to "lock" the channels into highly slowed activation kinetics that were similar to those of KCNQ2 A/V channels after depolarized conditioning prepulses; such slow kinetics were unaffected by the conditioning prepulse voltage (Fig. 4*A*); in particular, the activation time constants at 0 mV were 723 ± 241 and 655 ± 123 ms when conditioning prepulses of −100 or −60 mV, respectively, preceded the 0 mV test pulse ($n = 4–7$; $p > 0.05$).

Gating kinetics of several K^+ channels can be profoundly affected by changes in the extracellular concentrations of monovalent and divalent cations (Silverman et al., 2000; Consiglio and Korn, 2004). The described changes in current activation kinetics introduced by the KCNQ2 A/V mutation did not appear to be affected by an increase (from 5 to 50 mM) in the extracellular concentration of K^+ ions ($[K^+]_e$) or by the removal of extracellular Mg^{2+} ions ($[Mg^{2+}]_e$). In fact, when measured at +40 mV, the $A_f/A_f + A_s$ amplitude ratio of KCNQ2 A/V channels were, respectively, 0.62 ± 0.03, 0.64 ± 0.06, and 0.54 ± 0.06 when the holding voltage was −90 mV and 0.37 ± 0.03, 0.34 ± 0.07, and 0.28 ± 0.01 when the test potential was preceded by a 3 s prepulse to −60 mV in control conditions with 5 $[K^+]_e$ and 1 $[Mg^{2+}]_e$, or with 50 mM $[K^+]_e$ and 1 $[Mg^{2+}]_e$, or with 5 mM $[K^+]_e$ and 0 mM $[Mg^{2+}]_e$, respectively ($n = 3–10$ cells tested in each experimental condition; $p > 0.05$).

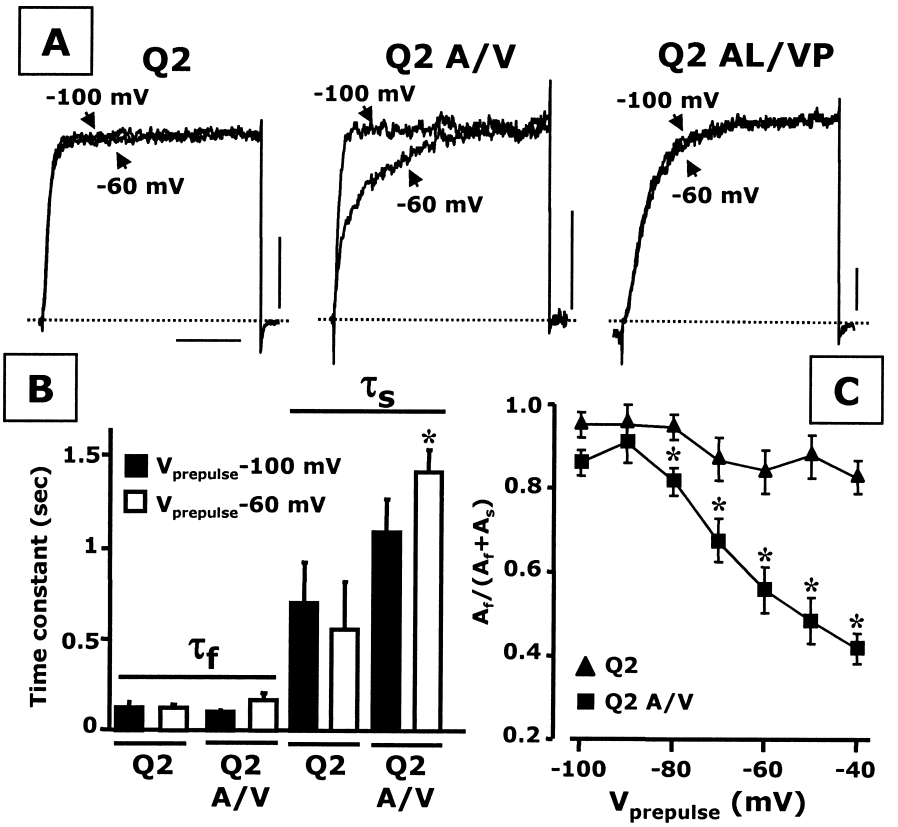

Figure 4. Current activation kinetics of KCNQ2 A/V channels depend on prepulse membrane voltage. ***A***, Representative current traces elicited by depolarizing pulses to 0 mV preceded by 3 s conditioning pulses at −100 or −60 mV, as indicated, from KCNQ2 (Q2), KCNQ2 A/V (Q2 A/V), and KCNQ2 AL/VP (Q2 AI/VP) channels. Current scale, 200 pA; time scale, 1 s. ***B***, Activation τ_f and τ_s values at 0 mV for KCNQ2 ($n = 3–5$) and KCNQ2 A/V ($n = 6–11$) channels obtained after −100 mV (filled bars) or −60 mV (empty bars) conditioning pulses of 3 s duration. The asterisk denotes a KCNQ2 A/V value significantly different ($p < 0.05$) from the corresponding KCNQ2 value. ***C***, Relative amplitudes of the fast and slow current activation components, expressed as $A_f/A_f + A_s$, as a function of the conditioning prepulse voltage ($V_{prepulse}$) for KCNQ2 and KCNQ2 A/V channels. Asterisks denote KCNQ2 A/V values significantly different from the corresponding KCNQ2 values ($p < 0.05$).

The described mutations in S_4 did not modify current sensitivity to the extracellular exposure to the pore blocker tetraethylammonium (TEA_e). In fact, the percentage of current inhibited at 0 mV by 0.3 mM TEA_e in homomeric KCNQ2, KCNQ2 A/V, and KCNQ2 AL/VP channels was 63 ± 9, 63 ± 1, and 61 ± 4%, respectively; 3 mM TEA_e inhibited the current carried by the same channels by 89 ± 2, 84 ± 6, and 90 ± 2%, respectively ($p > 0.05$) (Fig. 5*A*). Moreover, the exposure to the KCNQ channel activator retigabine (10 μM) caused similar leftward shifts in the voltage dependence of activation for KCNQ2, KCNQ2 A/V, and KCNQ2 AL/VP channels (by 19 ± 2, −18 ± 2, and −16 ± 1 mV, respectively) (Fig. 5*A*); the effects of both 3 mM TEA and 10 μM retigabine were fully reversible after washout. Interestingly, when KCNQ2 A/V channels were activated by square pulses to depolarizing potentials, retigabine was found to markedly slow down current activation kinetics (Fig. 5*B*). At 0 mV membrane potential, KCNQ2 A/V activation τ_f was increased, whereas the $A_f/A_f + A_s$ ratio was decreased by 10 μM retigabine exposure (Fig. 5*C*,*D*). Furthermore, hyperpolarizing prepulses up to −100 mV were unable to recover fast gating in KCNQ2 A/V channels during retigabine exposure (Fig. 5*D*). However, current activation kinetics of KCNQ2 (Fig. 5) and KCNQ2 AL/VP channels (data not shown) were unaffected by 10 μM retigabine.

Steady-state and kinetic properties of the macroscopic currents formed by KCNQ2 and KCNQ2 A/V subunits expressed heteromerically with KCNQ3 subunits

KCNQ2 subunits are thought to assemble with KCNQ3 subunits to form I_{KM} at most neuronal sites (Wang et al., 1998; Cooper et al., 2000). When compared with homomeric KCNQ2 channels, heteromeric KCNQ2+KCNQ3 channels displayed a reduced TEA_e sensitivity; such reduction was unaffected by the A/V mutation in KCNQ2. In fact, the percentage of current at 0 mV inhibited by 0.3 and 3 mM TEA_e was 9 ± 4 and 52 ± 6% or 9 ± 3 and 51 ± 9% in heteromeric KCNQ2+KCNQ3 or KCNQ2 A/V+KCNQ3 channels, respectively. In addition, the current density similarly increased by approximately threefold when either KCNQ2 or KCNQ2 A/V subunits were coexpressed with KCNQ3 subunits (102 ± 9 and 97 ± 12 pA/pF, respectively). These results suggested that the A/V mutation did not interfere with KCNQ2 subunit incorporation into heteromeric channels with KCNQ3 subunits. As shown in Figure 6*A*, heteromeric channels composed of KCNQ2 A/V+KCNQ3 subunits, when compared with KCNQ2+KCNQ3 channels, displayed gating changes qualitatively similar to those of homomeric KCNQ2 A/V channels; in fact, the $V_{1/2}$ and the slopes (k) were −20.6 ± 1.2 and −47.9 ± 1.3 mV, and 12.9 ± 0.9 and 8.6 ± 1.1 mV/*e*-fold, respectively, for KCNQ2 A/V+KCNQ3 and KCNQ2+KCNQ3 heteromeric channels ($n = 3$; $p < 0.05$ for both parameters) (Fig.

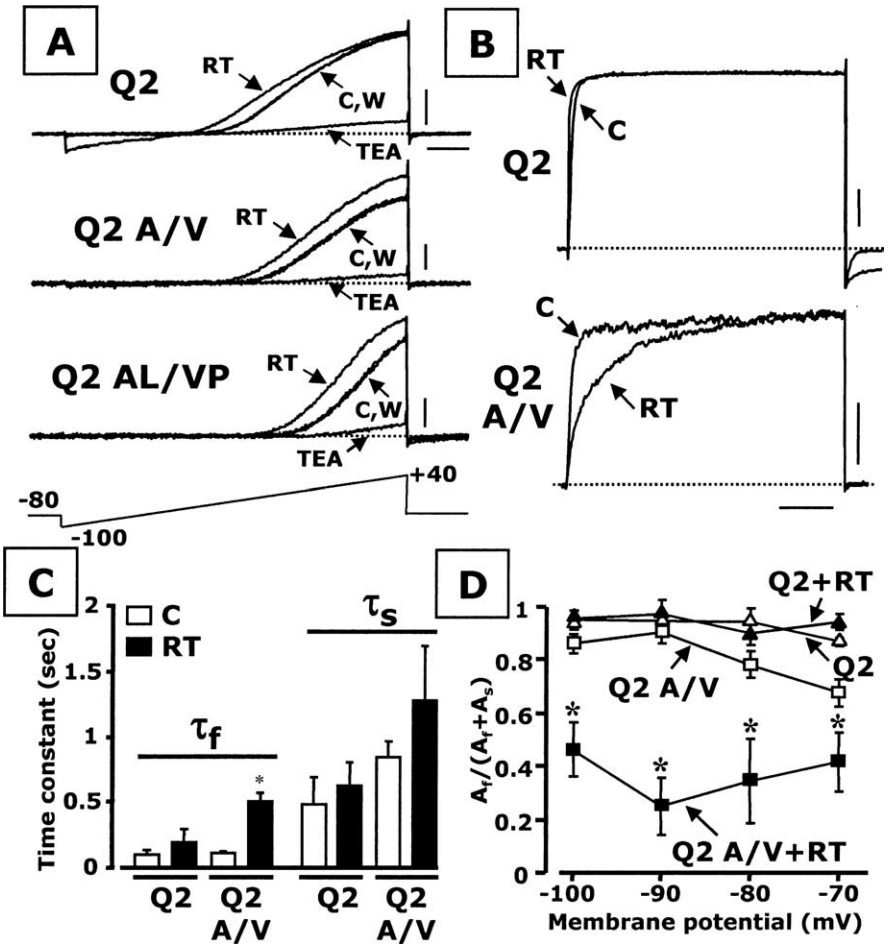

Figure 5. Retigabine delays current activation kinetics of KCNQ2 A/V channels. ***A***, Current responses from KCNQ2 (Q2), KCNQ2 A/V (Q2 A/V), and KCNQ2 AL/VP (Q2 AL/VP) channels, as indicated, to membrane voltage ramps from −100 to +40 mV (ramp speed, 116.6 mV/s; ramp frequency, 0.08 Hz). After recording the current responses in control conditions (C), the cells were subsequently exposed to 3 mM TEA (1 min), followed by washout (3 min), and to 10 μM retigabine (RT; 3 min), before final washout (W). Current scales, 500 pA for Q2, 200 pA for Q2 A/V and Q2 AL/VP; time scale, 200 ms. ***B***, Representative current traces elicited by depolarizing pulses to 0 mV preceded by 3 s conditioning pulses at −100 mV for KCNQ2 and KCNQ2 A/V channels before (C) or after 3 min of exposure to 10 μM RT, as indicated. Current scales, 500 pA for KCNQ2 or 200 pA for KCNQ2 A/V; time scale, 1 s. ***C***, Activation τ_f and τ_s values for KCNQ2 ($n = 4$) and KCNQ2 A/V ($n = 3$) channels (0 mV test pulse; 3 s conditioning pulse at −100 mV) recorded in C (empty bars) or after exposure to 10 μM RT (filled bars). The asterisk denotes a value significantly different ($p < 0.05$) from the corresponding control. ***D***, Relative amplitudes of the fast and slow current activation components, expressed as $A_f/A_f + A_s$, as a function of the conditioning prepulse voltage ($V_{prepulse}$) for KCNQ2 (triangles; $n = 4$) and KCNQ2 A/V channels (squares; $n = 3$), before (empty symbols) or after (filled symbols) retigabine exposure. Asterisks denote values (Q2 A/V+RT) significantly different ($p < 0.05$) from the corresponding controls (Q2 A/V no RT).

6*A*). Furthermore, current activation kinetics of heteromeric channels formed by KCNQ2 A/V and KCNQ3 subunits depended on the prepulse voltage (Fig. 6*B*), being markedly slower when the test pulse was preceded by conditioning prepulses at −60 mV; in particular, when the currents carried by KCNQ2+KCNQ3 heteromeric channels were measured at 0 mV, τ_f, τ_s, and $A_f/A_f + A_s$ were 58 ± 6 ms, 1169 ± 631 ms, and 0.85 ± 0.04% after a conditioning pulse at −100 mV and 78 ± 10 ms, 878 ± 339 ms, and 0.78 ± 0.04% after a conditioning pulse at −60 mV. In contrast, for KCNQ2 A/V+KCNQ3 heteromeric channels, the same parameters were 104 ± 30 ms, 652 ± 222 ms, and 0.93 ± 0.04% after a conditioning pulse to −100 mV and 157 ± 50 ms, 1191 ± 186 ms, and 0.59 ± 0.04% after a conditioning pulse at −60 mV. Thus, both τ_s and $A_f/A_f + A_s$ ratios of KCNQ2 A/V+KCNQ3 heteromeric channels were significantly affected by the prepulse voltage ($p < 0.05$). To quantify the prepulse voltage dependence of the macroscopic currents, we integrated for each experimental group (KCNQ2, KCNQ2 A/V, KCNQ2+KCNQ3, and KCNQ2 A/V+KCNQ3 channels) the currents elicited by the 0 mV test pulse for both conditioning prepulses of −100 or −60 mV; the normalized difference between these values, expressed as percentage, indicates the amount of prepulse-dependent current. As shown in Figure 6*C*, KCNQ2 subunits carrying the A/V mutation, both in homomeric or heteromeric configuration with KCNQ3 subunits, introduced a qualitatively and quantitatively similar prepulse voltage dependence of the currents at 0 mV. However, no significant dependence on prepulse membrane voltage was observed for the currents carried by KCNQ2 subunits, either alone or in heteromeric configuration with KCNQ3 subunits (Fig. 6*C*).

Discussion

In the present study, we found a novel missense mutation in the *KCNQ2* gene in a family affected by BFNC; this mutation (A196V; A/V) involved an uncharged residue, conserved among all KCNQ members except for KCNQ3, located at the N-terminal end of the S_4 voltage sensor. Electrophysiological analysis of the functional changes prompted by this genetic variant revealed that KCNQ2 A/V subunits introduced dramatic gating changes with no concomitant modification in the amount of macroscopic current expressed. In fact, channels incorporating KCNQ2 A/V mutant subunits showed a decreased sensitivity to voltage, requiring stronger depolarizations to become activated. These gating changes reflect true mutation-induced modifications of channel behavior rather than being the consequence of the many potential artifacts associated with intracellular dialysis during whole-cell recordings, as suggested by the convergence of the results obtained from macroscopic and single-channel current measurements.

KCNQ2 channels display two open states with different opening kinetics (Selyanko and Brown, 1999). The present results revealed that, in KCNQ2 channels, the slower opening transition only accounted for <20% of the macroscopic currents at potentials above −40 mV; such slower transition was markedly enhanced in KCNQ2 A/V mutant channels, reaching up to 60% of the total current kinetics at more depolarized potentials. The introduction of a second mutation at the amino acid position immediately past the A196 residue, reproducing the double substitution AL/VP caused by a *KCNQ2* mutant allele from a different BFNC-affected family (Moulard et al., 2001), retained similar steady-state consequences on the opening voltage dependence; moreover, current activation kinetics of KCNQ2 AL/VP channels were markedly slowed down, causing the fast opening compo-

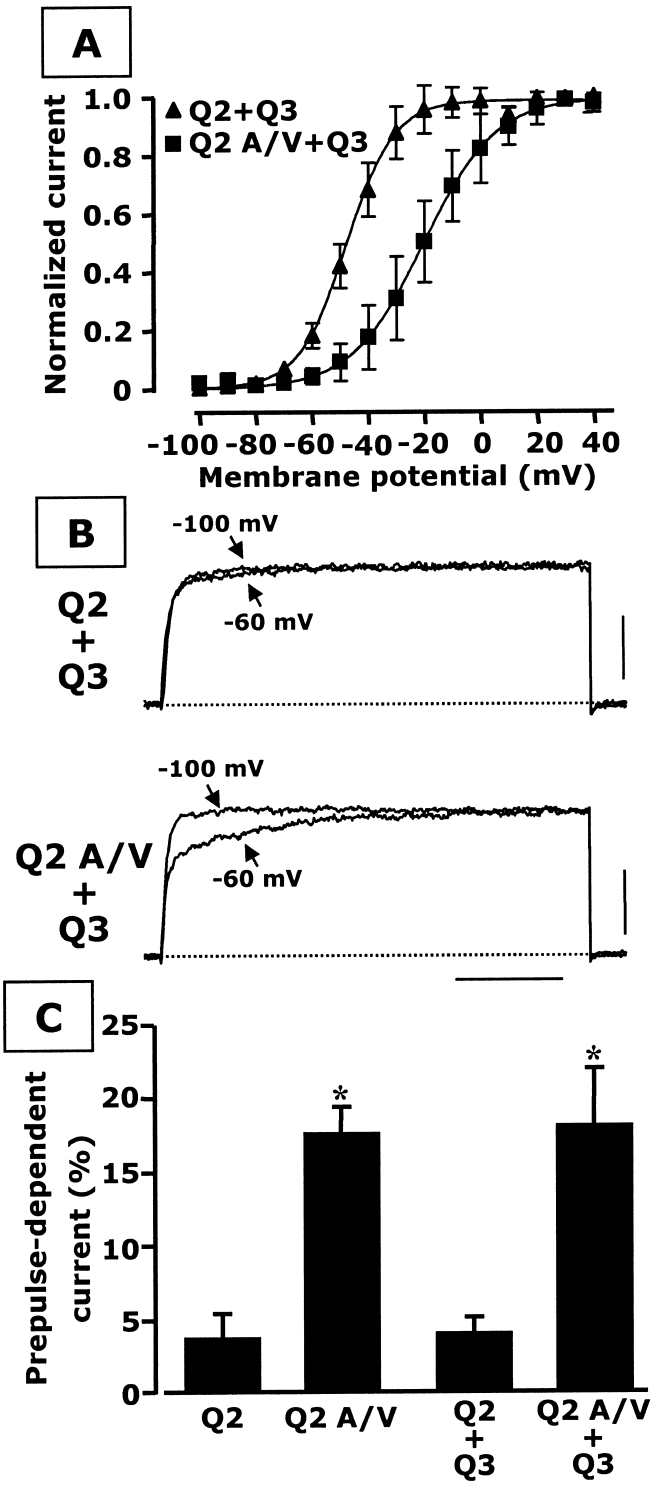

Figure 6. Steady-state and kinetic properties of heteromeric KCNQ2+KCNQ3 and KCNQ2 A/V+KCNQ3 channels. ***A***, Steady-state activation curves of KCNQ2+KCNQ3 (Q2+Q3) channels (1:1 cDNA ratio; $n = 3$) and KCNQ2 A/V+KCNQ3 (Q2 A/V+Q3) channels (1:1 cDNA ratio; $n = 8$). Continuous lines represent Boltzmann fits of the experimental data. ***B***, Representative current traces elicited by KCNQ2+KCNQ3 or KCNQ2 A/V+KCNQ3 heteromeric channels in response to a depolarizing pulse to 0 mV preceded by 3 s conditioning prepulses to −100 or −60 mV, as indicated by the arrows (current scale, 500 pA; time scale, 1 s). ***C***, Quantification of the prepulse-dependent current (for details, see Results) in KCNQ2 ($n = 4$), KCNQ2 A/V ($n = 8$), KCNQ2+KCNQ3 ($n = 3$), or KCNQ2 A/V+KCNQ3 ($n = 8$) channels. Asterisks denote KCNQ2 A/V and KCNQ2 A/V+KCNQ3 values significantly different from the corresponding controls (KCNQ2 and KCNQ2+KCNQ3, respectively) ($p < 0.05$).

nent to become undetectable. The biophysical results presented suggest that two kinetically distinct pathways exist for KCNQ2 channel opening and that, in A/V mutant channels, different prepulse potentials determine the distribution of channels between the two pathways. Whether these two open states result from different active configurations of the voltage sensors, as recently proposed by structural models comparing the $K_v1.2$ and K_vAP open configurations (Yarov-Yarovoy et al., 2006), or from more subtle structural changes unrelated to the position of the voltage-sensing domains, remains to be established.

Changes in voltage-dependent gating have been described previously in heterologously expressed channels carrying BFNC-causing mutations affecting charged residues in the S_4 segment of KCNQ2, namely the R207W (Dedek et al., 2001) and the R214W (Castaldo et al., 2002) substitutions. In contrast, the only other known BFNC mutation in KCNQ2 affecting an uncharged residue in S_4, the M208V substitution, has been shown not to affect the midpoint potential for current activation but rather to slightly increase the slope of the conductance to voltage curve and to lower the amount of expressed current (Singh et al., 2003), suggesting that the M208V mutation reduced I_{KM} function by mechanisms additional to gating alterations. However, the maximal probability of opening and the single-channel conductance of KCNQ2 A/V and KCNQ2 AL/VP mutant channels were similar to KCNQ2 channels; these results, together with the observation of an unaltered channel sensitivity to the pore blocker TEA and of an unchanged K^+/Na^+ selectivity ratio, suggested that changes in gating, rather than altered pore properties, mainly accounted for the impaired channel function caused by the mutations here investigated.

S_4 hydrophobic residues are involved in K^+ channel voltage-dependent gating (Lopez et al., 1991; McCormack et al., 1991), and it has been proposed that the gating differences between Shaker (K_v1) and Shaw (K_v3) channels are mainly accounted for by sequence differences with respect to S_4 uncharged amino acids (Smith-Maxwell et al., 1998). Uncharged amino acids also occupy the positions corresponding to A196 and L197 in the $K_v1.2$ voltage-gated K^+ channel (Fig. 1*C*) whose crystal structure has been recently solved (Long et al., 2005a). The intimate mechanism for voltage-sensing in K^+ channels is still an open matter of debate, and various models have been proposed to account for the multitude of results obtained with various techniques (Tombola et al., 2006). In particular, based on the structural data for $K_v1.2$ and K_vAP channels (Jiang et al., 2003), it has been proposed that membrane depolarization causes a paddle structure formed by two antiparallel α-helices (S_3 and S_4) to move outwardly, thus placing the positively charged residues of S_4 nearer to the extracellular side of the membrane (Long et al., 2005b). According to this paddle model, but also consistent with other gating models involving less pronounced S_4 conformational changes (Tombola et al., 2006), sequence modifications at the N-terminal end of the S_4 domain, the region affected by our mutations and in which the most important voltage-sensing arginines are located (Aggarwal and MacKinnon, 1996; Seoh et al., 1996), could interfere with the kinetics of S_4 movement during channel activation, ultimately leading to delayed pore opening.

Intriguingly, the A196V mutation introduced an unusual dependence of the macroscopic current activation kinetics on the prepulse voltage. The fact that the activation kinetics of K^+ channels depend on the preceding voltage was described >45 years ago in the squid axon by Cole and Moore (1960), who observed that K^+ current activation kinetics were delayed by prepulses to more negative membrane potentials. This phenomenon

prompted the suggestion that channel proteins transit through several closed conformations before opening and that transitions among the deepest closed states are rate-limiting for channel opening, a conclusion later confirmed also from gating current measurements in $K_v2.1$ (Taglialatela and Stefani, 1993) and in $K_v1.1$ channels (Bezanilla et al., 1994). However, our results show that the activation kinetics of KCNQ2 channels carrying the A196V mutation showed a phenomenon opposite to the Cole-Moore effect, namely an acceleration of gating kinetics by prepulses at hyperpolarizing voltages. Therefore, more depolarized prepulse potentials would allow mutant channels to preferentially populate an energetically favorable conformation in which the voltage sensors would be trapped in the inactive position, thus delaying their displacement to the active state, and, consequently, channel opening. Given that the mutation involved the substitution of a smaller and more polar alanine residue with a larger and more hydrophobic valine residue, it seems possible to speculate that, in such trapped configuration, the N-terminal end of the S_4 region encompassing the mutation resides in a more hydrophobic environment possibly represented by the membrane bilayer or by other protein regions.

Gating kinetics of several K^+ channels, including those of the Ether-a-go-go family (Terlau et al., 1996; Tang et al., 2000), are modulated by extracellular cations such as Mg^{2+}; moreover, the occupation of sites in the permeation pathway by K^+ ions is known to interfere with the motion of the gates (Ortega-Saenz et al., 2000). The fact that the gating properties of KCNQ2 A/V channels, similarly to KCNQ2 channels, were not affected by the removal of Mg^{2+} or by changing the concentrations of K^+ ions in the extracellular solution, suggested that the gating modifications introduced by the presently described A/V mutation in KCNQ2 did not involve an altered sensitivity to extracellular cations.

Gating changes may interfere with state-dependent drug binding. In particular, retigabine is a novel anticonvulsant that binds to an hydrophobic pocket of the activation gate formed by the S_5 and S_6 segments of neuronal KCNQ channels (Schenzer et al., 2005; Wuttke et al., 2005), thus stabilizing the open channel conformation. In KCNQ2 A/V channels, whose activation gating is slowed by depolarizing prepulses, retigabine favored the slower opening kinetics irrespectively of the prepulse voltage; this result highlights a reciprocal interaction between the voltage sensor and the inner gate before channel opening.

Intriguingly, the KCNQ2 double substitution AL/VP also removed the prepulse voltage dependence of channel opening kinetics and caused a marked slowing in the activation gating, suggesting that these two mutations represent a spectrum of functional derangement in which fast-gating kinetics could be introduced by hyperpolarizing prepulses in A196V singly substituted channels, whereas in the double A196V/L197P mutant channels, fast gating cannot be recovered by membrane voltages as negative as −100 mV.

The described changes in channel function prompted by the A196V mutation were not only observed in homomeric configuration but also in heteromeric configuration with KCNQ3 subunits. Given that I_{KM} seems to be mainly formed by heteromeric channels encompassing KCNQ2 and KCNQ3 subunits (Wang et al., 1998; Cooper et al., 2000), this suggests that the gating alterations introduced by the mutation may be relevant for the pathophysiology of the disease in the described family and provide a plausible explanation for its dominant hereditary transmission.

Mutation-induced I_{KM} impairment may occur by several mechanisms: some mutations preferentially alter the intracellular stability and trafficking of subunits (Soldovieri et al., 2006), whereas others interfere with their polarized neuronal targeting (Chung et al., 2006) or with their function once normally inserted into the plasma membrane (Dedek et al., 2001; Castaldo et al., 2002). Both the A196V and the A196V/L197P mutations appear to belong to the latter group, although the present results, obtained in non-neuronal context, cannot rule out a possible effect of the mutation on channel trafficking or localization.

Despite a wealth of studies addressing the molecular mechanisms responsible for BFNC pathogenesis, little is known on the cellular and developmental basis of the convulsive manifestation in the affected individuals. The gating changes introduced by the KCNQ2 A/V mutation herein investigated and, in particular, the novel dependence of current activation kinetics on the prepulse voltage, suggest that the mutation-induced functional derangement of I_{KM} may more prominently affect those neurons, such as GABAergic interneurons, firing at relatively high frequencies and whose resting membrane potential is more depolarized and closer to the threshold for spike initiation. The recent observation that, in hippocampal (Lawrence et al., 2006), striatal (Shen et al. 2005), and cerebellar (Forti et al., 2006) GABAergic interneurons, I_{KM} controls interspike interval, firing frequency, and overall network excitability, seems to lend support to this hypothesis. Moreover, during the first weeks of postnatal life, GABAergic neurons undergo age-dependent developmental switching from excitatory to inhibitory (Owens et al., 1996), suggesting that, in addition to changes in intrinsic excitability, also neuronal synchronization by excitatory synaptic activity may participate in BFNC pathogenesis (Okada et al., 2003); mutation-induced enhanced excitatory drive may ultimately lead to network hyperexcitability, thus predisposing to BFNC.

References

Aggarwal SK, MacKinnon R (1996) Contribution of the S4 segment to gating charge in the Shaker K+ channel. Neuron 16:1169–1177.

Bezanilla F, Perozo E, Stefani E (1994) Gating of Shaker K+ channels: II. The components of gating currents and a model of channel activation. Biophys J 66:1011–1021.

Biervert C, Schroeder BC, Kubisch C, Berkovic SF, Propping P, Jentsch TJ, Steinlein OK (1998) A potassium channel mutation in neonatal human epilepsy. Science 279:403–406.

Blackburn-Munro G, Jensen BS (2003) The anticonvulsant retigabine attenuates nociceptive behaviours in rat models of persistent and neuropathic pain. Eur J Pharmacol 460:109–116.

Boscia F, Annunziato L, Taglialatela M (2006) Retigabine and flupirtine exert neuroprotective actions in organotypic hippocampal cultures. Neuropharmacology 51:283–294.

Brown DA, Adams PR (1980) Muscarinic suppression of a novel voltage sensitive K^+ current in a vertebrate neurone. Nature 283:673–676.

Castaldo P, del Giudice EM, Coppola G, Pascotto A, Annunziato L, Taglialatela M (2002) Benign familial neonatal convulsions caused by altered gating of KCNQ2/KCNQ3 potassium channels. J Neurosci 22:RC199(1–6).

Charlier C, Singh NA, Ryan SG, Lewis TB, Reus BE, Leach RJ, Leppert M (1998) A pore mutation in a novel KQT-like potassium channel gene in an idiopathic epilepsy family. Nat Genet 18:53–55.

Chung HJ, Jan YN, Jan LY (2006) Polarized axonal surface expression of neuronal KCNQ channels is mediated by multiple signals in the KCNQ2 and KCNQ3 C-terminal domains. Proc Natl Acad Sci USA 103:8870–8875.

Cole KS, Moore JW (1960) Potassium ion current in the squid giant axon: dynamic characteristic. Biophys J 1:1–14.

Consiglio JF, Korn SJ (2004) Influence of permeant ions on voltage sensor function in the Kv2.1 potassium channel. J Gen Physiol 123:387–400.

Cooper EC, Aldape KD, Abosch A, Barbaro NM, Berger MS, Peacock WS, Jan YN, Jan LY (2000) Colocalization and coassembly of two human brain M-type potassium channel subunits that are mutated in epilepsy. Proc Natl Acad Sci USA 97:4914–4919.

Dedek K, Kunath B, Kananura C, Reuner U, Jentsch TJ, Steinlein OK (2001) Myokymia and neonatal epilepsy caused by a mutation in the voltage sensor of the KCNQ2 K+ channel. Proc Natl Acad Sci USA 98:12272–12277.

Engel Jr J (2001) A proposed diagnostic scheme for people with epileptic seizures and with epilepsy: report of the ILAE task force on classification and terminology. Epilepsia 42:796–803.

Forti L, Cesana E, Mapelli J, D'Angelo E (2006) Ionic mechanisms of autorhythmic firing in rat cerebellar Golgi cells. J Physiol (Lond) 574:711–729.

Halliwell JV, Adams PR (1982) Voltage-clamp analysis of muscarinic excitation in hippocampal neurons. Brain Res 250:71–92.

Horn R (1991) Estimating the number of channels in patch recordings. Biophys J 60:433–439.

Jiang Y, Lee A, Chen J, Ruta V, Cadene M, Chait BT, MacKinnon R (2003) X-ray structure of a voltage-dependent K+ channel. Nature 423:33–41.

Korsgaard MP, Hartz BP, Brown WD, Ahring PK, Strobaek D, Mirza NR (2005) Anxiolytic effects of maxipost (BMS-204352) and retigabine via activation of neuronal Kv7 channels. J Pharmacol Exp Ther 314:282–292.

Lawrence JJ, Saraga F, Churchill JF, Statland JM, Travis KE, Skinner FK, McBain CJ (2006) Somatodendritic Kv7/KCNQ/M channels control interspike interval in hippocampal interneurons. J Neurosci 26:12325–12338.

Li Y, Gamper N, Shapiro MS (2004a) Single-channel analysis of KCNQ K+ channels reveals the mechanism of augmentation by a cysteine-modifying reagent. J Neurosci 24:5079–5090.

Li Y, Langlais P, Gamper N, Liu F, Shapiro MS (2004b) Dual phosphorylations underlie modulation of unitary KCNQ K+ channels by Src tyrosine kinase. J Biol Chem 279:45399–45407.

Long SB, Campbell EB, Mackinnon R (2005a) Crystal structure of a mammalian voltage-dependent Shaker family K+ channel. Science 309:897–903.

Long SB, Campbell EB, Mackinnon R (2005b) Voltage sensor of Kv1.2: structural basis of electromechanical coupling. Science 309:903–908.

Lopez GA, Jan YN, Jan LY (1991) Hydrophobic substitution mutations in the S4 sequence alter voltage-dependent gating in Shaker K+ channels Neuron 7:327–336.

McCormack K, Tanouye MA, Iverson LE, Lin J-W, Ramaswami M, McCormack T, Campanelli JT, Mathew KM Rudy B (1991) A role for hydrophobic residues in the voltage-dependent gating of Shaker K+ channels. Proc Natl Acad Sci USA 88:2931–2935.

Main MJ, Cryan JE, Dupere JR, Cox B, Clare JJ, Burbidge SA (2000) Modulation of KCNQ2/3 potassium channels by the novel anticonvulsant retigabine. Mol Pharmacol 58:253–262.

Marrion NV (1997) Control of M-current. Annu Rev Physiol 59:483–504.

Martire M, Castaldo P, D'Amico M, Preziosi P, Annunziato L, Taglialatela M (2004) M channels containing KCNQ2 subunits modulate norepinephrine, aspartate, and GABA release from hippocampal nerve terminals. J Neurosci 24:592–597.

Miraglia del Giudice E, Coppola G, Scuccimarra G, Cirillo G, Bellini G, Pascotto A (2000) Benign familial neonatal convulsion (BFNC) resulting from mutation of the KCNQ2 voltage sensor. Eur J Hum Genet 8:994–998.

Moulard B, Picard F, le Hellard S, Agulhon C, Weiland S, Favre I (2001) Ion channel variation causes epilepsies. Brain Res Rev 36:275–284.

Okada M, Zhu G, Hirose S, Ito KI, Murakami T, Wakui M, Kaneko S (2003) Age-dependent modulation of hippocampal excitability by KCNQ-channels. Epilepsy Res 53:81–94.

Ortega-Saenz P, Pardal R, Castellano A, Lopez-Barneo J (2000) Collapse of conductance is prevented by a glutamate residue conserved in voltage-dependent K(+) channels. J Gen Physiol 116:181–190.

Otto M, Cepek L, Ratzka P, Doehlinger S, Boekhoff I, Wiltfang J, Irle E, Pergande G, Ellers-Lenz B, Windl O, Kretzschmar HA, Poser S, Prange H (2004) Efficacy of flupirtine on cognitive function in patients with CJD: a double-blind study. Neurology 62:714–718.

Owens DF, Boyce LH, Davis MB, Kriegstein AR (1996) Excitatory GABA responses in embryonic and neonatal cortical slices demonstrated by gramicidin perforated-patch recordings and calcium imaging. J Neurosci 16:6414–6423.

Passmore GM, Selyanko AA, Mistry M, Al-Qatari M, Marsh SJ, Matthews EA, Dickenson AH, Brown TA, Burbidge SA, Main M, Brown DA (2003) KCNQ/M currents in sensory neurons: significance for pain therapy. J Neurosci 23:7227–7236.

Richter A, Sander SE, Rundfeldt C (2006) Antidystonic effects of Kv7 (KCNQ) channel openers in the dt sz mutant, an animal model of primary paroxysmal dystonia. Br J Pharmacol 149:747–753.

Rogawski MA (2000) KCNQ2/KCNQ3 K^+ channels and the molecular pathogenesis of epilepsy: implications for therapy. Trends Neurosci 23:393–398.

Ronen GM, Rosales TO, Connolly M, Anderson VE, Leppert M (1993) Seizure characteristics in chromosome 20 benign familial neonatal convulsions. Neurology 43:1355–1360.

Rostock A, Tober C, Rundfeldt C, Bartsch R, Engel J, Polymeropoulos EE, Kutscher B, Loscher W, Honack D, White HS, Wolf HH (1996) D-23129: a new anticonvulsant with a broad spectrum activity in animal models of epileptic seizures. Epilepsy Res 23:211–223.

Rundfeldt C, Netzer R (2000) The novel anticonvulsant retigabine activates M-currents in Chinese hamster ovary-cells transfected with human KCNQ2/3 subunits. Neurosci Lett 282:73–76.

Schenzer A, Friedrich T, Pusch M, Saftig P, Jentsch TJ, Grotzinger J, Schwake M (2005) Molecular determinants of KCNQ (Kv7) K+ channel sensitivity to the anticonvulsant retigabine. J Neurosci 25:5051–5060.

Selyanko AA, Brown DA (1999) M-channel gating and simulation. Biophys J 77:701–713.

Seoh SA, Sigg D, Papazian DM, Bezanilla F (1996) Voltage-sensing residues in the S2 and S4 segments of the Shaker K+ channel. Neuron 16:1159–1167.

Shen W, Hamilton SE, Nathanson NM, Surmeier DJ (2005) Cholinergic suppression of KCNQ channel currents enhances excitability of striatal medium spiny neurons. J Neurosci 25:7449–7458.

Shieh CC, Coghlan M, Sullivan JP, Gopalakrishnan M (2000) Potassium channels: molecular defects, diseases, and therapeutic opportunities. Pharmacol Rev 52:557–593.

Silverman WR, Tang CY, Mock AF, Huh KB, Papazian DM (2000) Mg2+ modulates voltage-dependent activation in ether-a-go-go potassium channels by binding between transmembrane segments S2 and S3. J Gen Physiol 116:663–677.

Singh NA, Charlier C, Stauffer D, Dupont BR, Leach RJ, Melis R, Ronen GM, Bjerre I, Quattlebaum T, Murphy JV, McHarg ML, Gagnon D, Rosales TO, Peiffer A, Anderson VE, Leppert M (1998) A novel potassium channel gene, KCNQ2, is mutated in an inherited epilepsy of newborns. Nat Genet 18:25–29.

Singh NA, Westenskow P, Charlier C, Pappas C, Leslie J, Dillon J, The BFNC Physician Consortium, Anderson VE, Sanguinetti MC, Leppert M (2003) KCNQ2 and KCNQ3 potassium channel genes in benign familial neonatal convulsions: expansion of the functional and mutation spectrum. Brain 126:1–12.

Smith-Maxwell CJ, Ledwell JL, Aldrich RW (1998) Uncharged S4 residues and cooperativity in voltage-dependent potassium channel activation. J Gen Physiol 111:421–439.

Soldovieri MV, Castaldo P, Iodice L, Miceli F, Barrese V, Bellini G, Miraglia del Giudice E, Pascotto A, Bonatti S, Annunziato L, Taglialatela M (2006) Decreased subunit stability as a novel mechanism for potassium current impairment by a KCNQ2 C-terminus mutation causing benign familial neonatal convulsions. J Biol Chem 281:418–428.

Steinlein OK (1998) New insights into the molecular and genetic mechanisms underlying idiopathic epilepsies. Clin Genet 54:169–175.

Taglialatela M, Stefani E (1993) Gating currents of the cloned delayed rectifier K^+ channel DRK1. Proc Natl Acad Sci USA 90:4758–4762.

Tang CY, Bezanilla F, Papazian DM (2000) Extracellular Mg2+ modulates slow gating transitions and the opening of *Drosophila* ether-a-Go-Go potassium channels. J Gen Physiol 115:319–338.

Terlau H, Ludwig J, Steffan R, Pongs O, Stuhmer W, Heinemann SH (1996) Extracellular Mg2+ regulates activation of rat eag potassium channel. Pflügers Arch 432:301–312.

Tombola F, Pathak MM, Isacoff EY (2006) How does voltage open an ion channel? Annu Rev Cell Dev Biol 22:23–52.

Wang HS, Pan Z, Shi W, Brown BS, Wymore RS, Cohen IS, Dixon JE, McKinnon D (1998) KCNQ2 and KCNQ3 potassium channel subunits: molecular correlates of the M-channel. Science 282:1890–1893.

Wickenden AD, Yu W, Zou A, Jegla T, Wagoner PK (2000) Retigabine, a novel anticonvulsant, enhances activation of KCNQ2/3 potassium channels. Mol Pharmacol 58:591–600.

Wuttke TV, Seebohm G, Bail S, Maljevic S, Lerche H (2005) The new anticonvulsant retigabine favors voltage-dependent opening of the Kv7.2 (KCNQ2) channel by binding to its activation gate. Mol Pharmacol 67:1009–1017.

Yarov-Yarovoy V, Baker D, Catterall WA (2006) Voltage sensor conformations in the open and closed states in ROSETTA structural models of K+ channels. Proc Natl Acad Sci USA 103:7292–7297.